Impact of GCM structure uncertainty on hydrological processes in an arid area of China

Gonghuan Fang, Jing Yang, Yaning Chen, Zhi Li and Philippe De Maeyer

ABSTRACT

Quantifying the uncertainty sources in assessment of climate change impacts on hydrological processes is helpful for local water management decision-making. This paper investigated the impact of the general circulation model (GCM) structural uncertainty on hydrological processes in the Kaidu River Basin. Outputs of 21 GCMs from the Coupled Model Intercomparison Project Phase 5 (CMIP5) under two representative concentration pathway (RCP) scenarios (i.e., RCP4.5 and RCP8.5), representing future climate change under uncertainty, were first bias-corrected using four precipitation and three temperature methods and then used to force a well-calibrated hydrological model (the Soil and Water Assessment Tool, SWAT) in the study area. Results show that the precipitation will increase by 3.1%–18% and 7.0%–22.5%, the temperature will increase by 2.0 °C–3.3 °C and 4.2 °C–5.5 °C and the streamflow will change by −26% to 3.4% and −38% to −7% under RCP4.5 and RCP8.5, respectively. Timing of snowmelt will shift forward by approximately 1–2 months for both scenarios. Compared to RCPs and bias correction methods, GCM structural uncertainty contributes most to streamflow uncertainty based on the standard deviation method (55.3%) while it is dominant based on the analysis of variance approach (94.1%).

Key words | climate change, GCM structural uncertainty, hydrological modelling, uncertainty decomposition

Gonghuan Fang
Jing Yang (corresponding author)
Yaning Chen
Zhi Li
State Key Laboratory of Desert and Oasis Ecology,
Xinjiang Institute of Ecology and Geography,
Chinese Academy of Sciences,
Xinjiang 830011,
China
E-mail: *yangjing@ms.xjb.ac.cn*

Jing Yang
National Institute of Water and Atmospheric Research,
Christchurch 8011,
New Zealand

Gonghuan Fang
Philippe De Maeyer
Department of Geography,
Ghent University,
Ghent 9000,
Belgium;
Sino-Belgian Joint Laboratory for Geo-Information,
Urumqi 830011,
China;
and
Sino-Belgian Joint Laboratory for Geo-Information,
Ghent 9000,
Belgium

INTRODUCTION

The Intergovernmental Panel on Climate Change (IPCC 2014) stated that the precipitation and temperature patterns would significantly change by the end of the 21st century. Climate change has a wide and profound impact on hydrological processes. Changes in hydrological processes and increased extreme events (e.g., drought and flood) have been detected and have exerted significant impacts on ecological and social systems (IPCC 2014). Therefore, understanding the hydro-climatic effects of future climate change is critical to local water management, especially for arid regions, where hydrological changes are more sensitive to climate change than those humid regions.

When accessing the impact of future climate change on hydrology, climate models are often coupled with hydrological models (HMs) to predict future changes in hydrological processes (Liu *et al.* 2010; Ficklin *et al.* 2013; IPCC 2014). Climate change projected by state-of-the-art general circulation models (GCMs) suggested a warming temperature trend along with seasonally and spatially varying precipitations for the 21st century (Reyers *et al.* 2013). As uncertainty is inherited in modelling, it is necessary to consider the uncertainties from GCMs, climate variable downscaling and hydrological modelling (Graham *et al.* 2007; Jiang *et al.* 2007; Chen *et al.* 2011, 2012) in local impact studies. Previous studies have investigated different uncertainty sources, and

doi: 10.2166/nh.2017.227

most of them noted that GCMs are one of the greatest sources of uncertainty in assessing climate change impact on hydrological processes (Horton *et al.* 2006; Wilby & Harris 2006; Graham *et al.* 2007; Chen *et al.* 2011, 2016; Dobler *et al.* 2012; Bosshard *et al.* 2013; Lung *et al.* 2013; Exbrayat *et al.* 2014), although uncertainty from HMs was also important over many areas of the world (Hagemann *et al.* 2013). More specifically, major contributors to uncertainty depend on the assessed hydrological variables (Booij 2005; Chen *et al.* 2011; Gampe *et al.* 2016; Shrestha *et al.* 2016) and the assessed watersheds (Finger *et al.* 2012; Lutz *et al.* 2013; Ragettli *et al.* 2013; Addor *et al.* 2014; Huss *et al.* 2014; Vidal *et al.* 2016). Methodology used for uncertainty decomposition includes qualitative visual interpretation of the prediction spread (Wilby & Harris 2006; Graham *et al.* 2007; Chen *et al.* 2011) and the quantitative standard deviation method (Xu & Xu 2012) and analysis of variance (ANOVA) approach (Bosshard *et al.* 2013; Addor *et al.* 2014; Duethmann *et al.* 2016). Although these studies have been conducted in many regions throughout the world, the differences between these uncertainty decomposition methods have been seldom compared.

The Tienshan Mountains, 'water tower' of central Asia, are the main water sources and ecological barriers, and very typical in terms of the dry and alpine continental climate characteristics together with data scarcity. The Kaidu River, a typical watershed located in the south slope of the Tienshan Mountains, is one of the headwaters of the Tarim River, the largest endorheic basin in China. Understanding future hydrological processes and their related uncertainty help the sustainable development of countries along the 'Silk Road' (Li *et al.* 2015). In the literature, most studies in this area have focused on historical hydrological events (Shi *et al.* 2007; Liu *et al.* 2010; Piao *et al.* 2010; Chen 2014; Rumbaur *et al.* 2015). Although there have been some investigations for future scenarios (Liu *et al.* 2010, 2011; Sorg *et al.* 2012; Fang *et al.* 2015a; Xu *et al.* 2016), few of them (Duethmann *et al.* 2016) quantified the uncertainty sources. Characterizing the uncertainty sources is of high importance for a valid interpretation of the results.

This paper aims to investigate the impact of climate change on the hydrological system and assess the impact of GCM structural uncertainty on hydrological processes. To this end, a cascade of a GCM ensemble, downscaling methods and a HM were used to simulate future hydrological processes. Three main questions are addressed: (1) How will the future climate and hydrological processes change in this arid mountainous region? (2) Which one of the following issues contributes most to future hydrological processes: GCM structure uncertainty, representative concentration pathways (RCPs) or downscaling methods? (3) Do different uncertainty decomposition methods produce different results? Understanding these issues will enable us to better assess future hydrological changes and related uncertainties. The paper is organized as follows: the section below introduces the study area; the next section describes the cascade of the GCM ensemble, bias correction methods, HM and the methodology on how to decompose the uncertainty sources; a results and discussion section follows and the final section drawing conclusions.

STUDY AREA

The Kaidu River Basin (Figure 1), with a drainage area of 18,634 km^2 above the Dashankou hydrological station, is one of the four headwaters of the Tarim River. It originates in the Tienshan Mountains. Recharged mainly by rainfall and snowmelt (SM), the Kaidu River provides 42×10^8 m^3 amount of water for agricultural irrigation and ecological water conveyance for the lower reaches of the Tarim River, which is crucial to the local eco-environmental and economic development. The altitude ranges from 1,340 m to 4,796 m above sea level (a.s.l.) with an average elevation of 2,995 m and average slope of 23%. This watershed has a temperate continental climate with alpine characteristics. The average annual temperature at the Bayanbulak meteorological station is $-4.1\,^{\circ}C$ and annual precipitation is 278 mm; precipitation generally falls as rain from May to September and as snow from October to April of the next year. The average daily flow at the Dashankou hydrological station is around 120 m^3/s (equivalent to 201 mm runoff), ranging from 15 m^3/s to 973 m^3/s.

DATA AND METHODOLOGY

Figure 2 presents the framework for the hydrological modelling under future climate change. First, daily climate

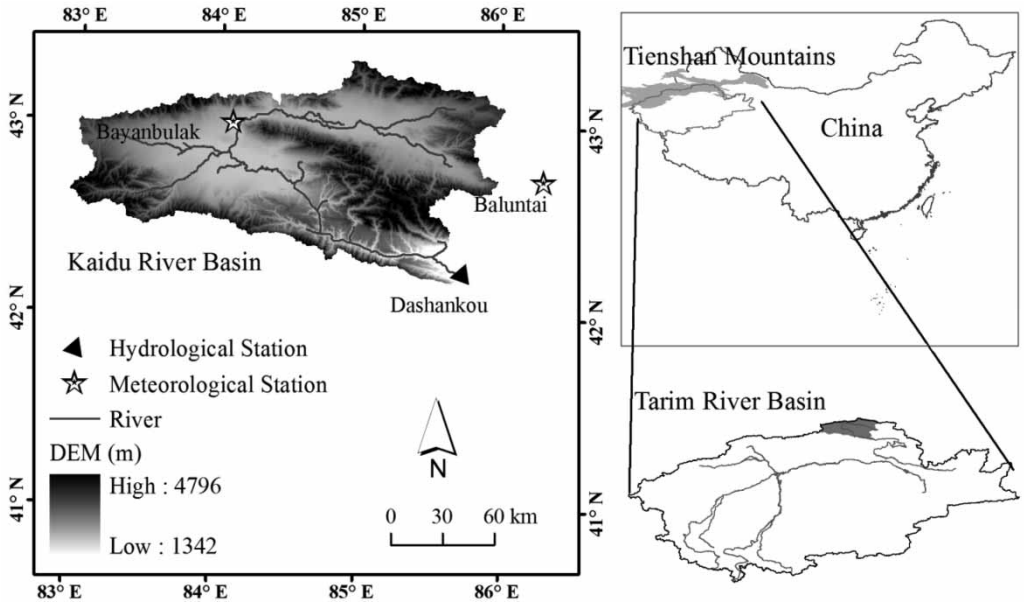

Figure 1 | The topography, river system, meteorological stations (Bayanbulak and Baluntai) and hydrological station (Dashankou) of the Kaidu River Basin together with its location in the Tarim River Basin (bottom right) and China (top right).

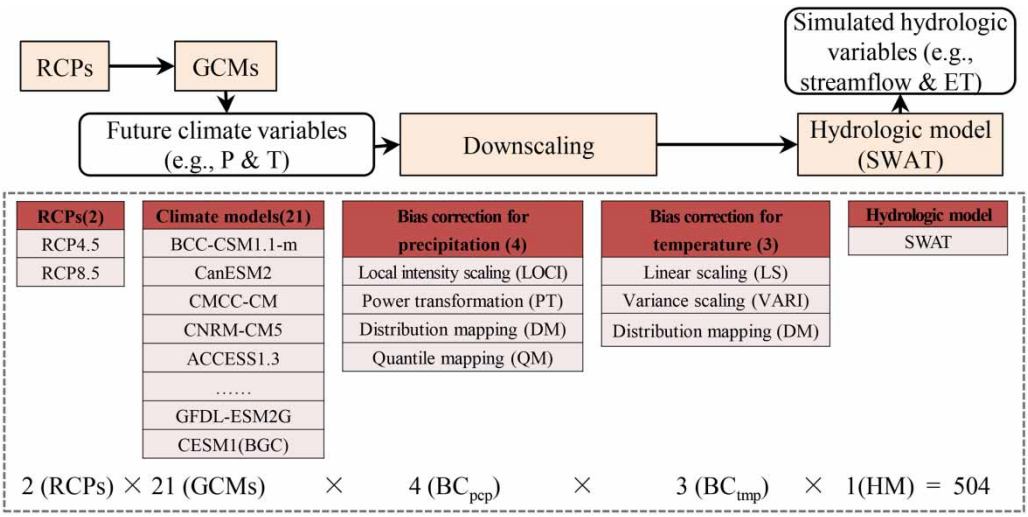

Figure 2 | Framework to study the future climate impact on hydrological processes. The dashed box shows different RCPs, GCMs, bias correction methods for precipitation and temperature, and the HM.

predictions from 21 GCM models from CMIP5 (Coupled Model Intercomparison Project Phase 5) under RCP4.5 and RCP8.5 were downloaded (http://cmip-pcmdi.llnl.gov/cmip5/; IPCC 2013), and then these grid-based climate predictions were downscaled/bias-corrected to the station scale using four precipitation (BC_{pcp}) and three temperature (BC_{tmp}) bias correction methods. These bias-corrected climatic variables were used to force the well-calibrated HM of the Soil and Water Assessment Tool (SWAT). Compared to other sources (e.g., model parameter, model structure), meteorological input contributes to the largest part of uncertainties in hydrological modelling (Wilby & Harris 2006; Graham *et al.* 2007; Chen *et al.* 2011, 2016; Bosshard *et al.* 2013), therefore, we only used one HM in this

study. In total, there were 504 hydrological simulations from 504 different combined meteorological inputs (i.e., different combinations of 21 GCMs, 2 RCPs, 4 BC_{pcp}s and 3 BC_{tmp}s), as shown in Figure 2.

GCMs and RCPs

The state-of-the-art climate change projections of 21 GCMs under two emission scenarios (RCP4.5 and RCP8.5) were used as climatic data in this study (Table 1). These models are from over 20 institutes or universities. Of all GCM simulated climate variables, daily precipitation, and maximum and minimum temperatures from 1975 to 2099 were used.

RCP4.5 (lower emission scenario) is a stabilization scenario with the total radiative forcing rising until 2070, which will remain stable at 4.5 W/m^2. In contrast, RCP8.5 (higher emission scenario) is a continuously rising radiative forcing pathway (at a target of 8.5 W/m^2 in 2,100) with a further enhanced residual circulation and significant CH_4 increase (Van Vuuren *et al.* 2011). RCP4.5 and RCP8.5 are equivalent to B1 and A2 of the Special Report on Emission Scenarios (SRES).

Table 1 | Information about the GCM ensemble used in this study

No.	Modelling centre	Model	Institution
1	BCC	BCC-CSM1.1-m	Beijing Climate Center, China Meteorological Administration
2	CCCma	CanESM2	Canadian Centre for Climate Modelling and Analysis
3	CMCC	CMCC-CM	Euro-Mediterranean Centre on Climate Change
4	CNRM-CERFACS	CNRM-CM5	CNRM (National Centre for Meteorological Research), CERFACS (European Center for Research and Advanced Training in Scientific Computation)
5	CSIRO-BOM	ACCESS1.3	CSIRO (Commonwealth Scientific and Industrial Research Organisation, Australia), and BOM (Bureau of Meteorology, Australia)
6	CSIRO-QCCCE	CSIRO-Mk3.6	Commonwealth Scientific and Industrial Research Organisation/Queensland Climate Change Centre of Excellence
7	GCESS	BNU-ESM	College of Global Change and Earth System Science, Beijing Normal University
8	INM	INM-CM4	Institute for Numerical Mathematics
9	IPSL	IPSL-CM5B-LR	Institute Pierre-Simon Laplace
10	LASG-CESS	FGOALS-g2	LASG, Institute of Atmospheric Physics, Chinese Academy of Sciences; and CESS, Tsinghua University
11	MIROC	MIROC5	Atmosphere and Ocean Research Institute (The University of Tokyo), National Institute for Environmental Studies, and Japan Agency for Marine-Earth Science and Technology
12	MIROC	MIROC-ESM	Atmosphere and Ocean Research Institute (The University of Tokyo), National Institute for Environmental Studies, and Japan Agency for Marine-Earth Science and Technology
13	MOHC	HadGEM2-ES	Met Office Hadley Centre
14	MPI-M	MPI-ESM-LR	Max Planck Institute for Meteorology
15	MRI	MRI-ESM1	Meteorological Research Institute
16	NASA GISS	GISS-E2-R	NASA Goddard Institute for Space Studies
17	NCAR	CCSM4	National Center for Atmospheric Research
18	NCC	NorESM1-M	Norwegian Climate Centre
19	NOAA GFDL	GFDL-CM3	Geophysical Fluid Dynamics Laboratory
20	NOAA GFDL	GFDL-ESM2G	Geophysical Fluid Dynamics Laboratory
21	NSF-DOE-NCAR	CESM1(BGC)	National Science Foundation, Department of Energy, National Center for Atmospheric Research

Downscaling/bias correction methods

To account for the low spatial resolution in GCM outputs, four BC_{pcp} and three BC_{tmp} methods were used to downscale the grid-based GCM outputs to the station scale (where there is a meteorological station). These correction methods are local intensity scaling (LOCI), power transformation (PT), distribution mapping (DM) and quantile mapping (QM) for precipitation as well as linear scaling (LS), variance scaling (VARI) and DM for temperature. These methods can be classified into mean-based (LS and LOCI), variance-based (PT and VARI) and distribution-based approaches (DM and QM). Table 2 briefly describes the characteristics of each method. The methods have been widely used in downscaling and bias correcting the climate model outputs (e.g., Schmidli *et al.* 2006; Fang *et al.* 2015b).

HM and model setup

SWAT (Arnold *et al.* 1998), developed at the Agriculture Research Service of the United States Department of Agriculture, has been widely used for comprehensive modelling of the impacts of management practices and climate change on hydrological processes at a watershed scale (e.g., Jayakrishnan *et al.* 2005; Singh *et al.* 2015; Awan *et al.* 2016; Tamm *et al.* 2016). To represent the spatial variability, a watershed is first disaggregated into subbasins and each subbasin is further divided into hydrological response units based on soil and land use data. For more details, refer to SWAT manuals (http://www.brc.tamus.edu/).

The SWAT model was successfully applied in the Kaidu River Basin (Fang *et al.* 2015c). The SWAT model was first set up with digital elevation model (DEM) (www2.jpl.nasa.gov/srtm/), land use (from the Environmental and Ecological Science Data Centre for West China), soil map (from Xinjiang Institute of Ecology and Geography, Chinese Academy of Sciences), and observed meteorological data (at two meteorological stations Bayanbulak and Baluntai, Figure 1; China Meteorological Data Sharing Service System), which form the base for estimating meteorological input for each subbasin with the elevation band method. Then, model parameters were calibrated with the observed streamflow data at Dashankou station (hydrological station in Figure 1) and good model performances were achieved for both calibration and validation periods, as shown in Table 3. More details of the SWAT model setup and calibration can be found in Fang *et al.* (2015c).

When studying the impact of climate change on flow extremes, we used average annual 3-day maximum high

Table 2 | Characteristics of bias correction methods for temperature and precipitation

Approach	Characteristics	Reference
Precipitation		
LOCI	It corrects the wet-day frequencies and intensities by setting all precipitation values less than a wet-day threshold to zeros	Schmidli *et al.* (2006) and Fang *et al.* (2015b)
PT	It adjusts the standard deviation of the precipitation series by producting a factor for each month	Teutschbein & Seibert (2012)
DM	To match the assumed distribution function of the raw data to that of the observations by assuming the raw and the observed precipitation follow the gamma distribution	Block *et al.* (2009) and Piani *et al.* (2010)
QM	It is non-parametric and is generally applicable for all possible distributions of precipitation without any assumption on its distribution	Themeßl *et al.* (2012) and Chen *et al.* (2013)
Temperature		
LS	To perfectly match the monthly average of corrected values with that of observed ones by adding a factor	Lenderink *et al.* (2007)
VARI	To correct both the mean and variance of temperature	Terink *et al.* (2010) and Teutschbein & Seibert (2012)
DM	To match the assumed distribution function of the raw data to that of the observations by assuming the raw and the observed temperatures follow normal distributions	Teutschbein & Seibert (2012)

Table 3 | Performance of SWAT model forced by the observed meteorological data

Statistics	NS	PBIAS	R^2
Daily streamflow (calibration period 1986–1989)	0.80	0.01%	0.80
Daily streamflow (validation period 1990–2002)	0.81	2.94%	0.81
3DMHF (validation period 1990–2002)	0.43	−19.6%	0.98
7DMLF (validation period 1990–2002)	0.72	7.5%	0.87

flow (3DMHF) and average annual 7-day minimum low flow (7DMLF), as used in Sanborn & Bledsoe (2006).

Quantification of uncertainties from GCMs, RCPs, BC_{pcp} and BC_{tmp}

To analyse the impact of climate change on hydrological processes, five periods are defined: 1986–2005 (control period), 2020–2039, 2040–2059, 2060–2079 and 2080–2099. For future changes of the precipitation, temperature and streamflow, we calculated the ensemble median and 25th and 75th percentiles instead of the mean value because these statistics have a lower sensitivity to outliers than the ensemble mean (Benestad 2004).

There have been several uncertainty quantification methods applied in climate change impact studies, as proposed in the 'Introduction'. Standard deviation and ANOVA approach are two quantitative methods commonly used in assessing the contributions of GCMs, downscaling methods, RCPs and HMs to the total variance of hydrological variables within an ensemble of climate models (Yip *et al.* 2011; Déqué *et al.* 2012; Gampe *et al.* 2016; Vidal *et al.* 2016). Here, we used these two methods to decompose the contributions of GCMs, RCPs, BC_{pcp} and BC_{tmp} to prediction uncertainty.

The model ensemble consists of 504 model runs (combinations of 21 GCMs, 2 RCPs, 4 BC_{pcp}s and 3 BC_{tmp}s, as in Figure 2). For each model run, the hydrological signal Y (i.e., relative change of a hydrological variable) of the future periods (i.e., 2020–2039, 2040–2059, 2060–2079 and 2080–2099) was calculated as:

$$Y = \frac{(Q^{FUT} - Q^{CTL})}{Q^{CTL}} \tag{1}$$

where Q^{FUT} and Q^{CTL} are values of a given hydrological variable at the future period and control period. The decomposition of its total uncertainty can be conducted by either the standard deviation or ANOVA.

Standard deviation method

In the standard deviation method, the uncertainty σ_A from source A can be derived as the mean standard deviation of the model ensemble by varying source A, while keeping other sources (denoted as $A\sim$ in the equation below) constant:

$$\sigma_A = \mu(\sigma(Y(A|A\sim))) \tag{2}$$

where $\mu(.)$ and $\sigma(.)$ represent the mean and the standard deviation operator. For example, the uncertainty from GCMs σ_{GCMs} can be obtained through Equation (2) by varying GCMs from 1st to 21st while keeping RCP, BC_{pcp} and BC_{tmp} constant.

ANOVA approach

When applying the ANOVA approach, each uncertainty source is taken as an 'effect' which has an influence on Y. The total sum of squares (SSQ_{tot}) can be decomposed into sums of squares of the individual uncertainty source, their interactions ($SSQ_{Interaction}$) and an error term SSE. In this study, we ignored the interactions and ANOVA is expressed as:

$$SSQ_{tot} = SSQ_{GCM} + SSQ_{RCP} + SSQ_{BCpcp} + SSQ_{BCtmp} + SSE \tag{3}$$

where SSQ_{GCM}, SSQ_{RCP}, SSQ_{BCpcp} and SSQ_{BCtmp} are sums of squares of GCM, RCP, BC_{pcp} and BC_{tmp}, respectively. As indicated by Bosshard *et al.* (2013) and Duethmann *et al.* (2016), variances calculated with Equation (3) are overestimated by a factor of $N_i/(N_i - 1)$ where N is the sample size of the ith source. Here we offset this by multiplying the uncertainty contribution with a factor f_i to keep the sum of SSQ_{GCM}, SSQ_{RCP}, SSQ_{BCpcp} and SSQ_{BCtmp} constant.

$$f_i = \frac{N_i}{N_i - 1} \times \frac{\sum_{i=1}^{I} SSQ_i}{\sum_{i=1}^{I} SSQ_i \times (N_i/(N_i - 1))} \tag{4}$$

Then, we can get the contribution η_i of the ith uncertainty source to the total ensemble uncertainty:

$$\eta_i = f_i \times \frac{SSQ_i}{\sum_{i=1}^{I} SSQ_i} \tag{5}$$

The signal-to-noise ratio (S/N) was used to quantitively reveal the robustness of the projected streamflow (Zhou & Yu 2006; Addor *et al.* 2014). Assume that $Y(n,t)$ is the relative changes of future streamflow from the nth simulation ($n = 1, 2, \ldots, 252$) at tth year ($t = 1, 2, \ldots, 40$) for 1986–2005 and 2080–2099 for RCP4.5 or RCP8.5, and the multisimulation mean at year t ($x_s(\mathrm{t}) = (1/N)\sum_{n=1}^{N} Y(n,t)$). The S/N can be represented by:

$$\frac{S}{N} = \frac{\sigma_{signal}}{\sigma_{noise}} \tag{6}$$

$$\sigma_{signal} = \sigma(x_s(\mathrm{t})), \text{ with } t = 1, 2, \ldots, 40 \tag{7}$$

$$\sigma_{noise} = \mu(\sigma_t(Y(n,t))) \text{ with } n = 1, 2, \ldots, 252, \text{ and } t = 1, 2, \ldots, 40 \tag{8}$$

The larger S/N is, the higher the credibility and more significant are the changes in the projected streamflow. Normally, $S/N > 1$ indicates that the projections are credible to a certain extent while $S/N < 1$ indicates low credibility or with unsignificant changes (Zhou & Yu 2006).

Further, the consistency of the simulations is estimated as the ratio of the number of simulations with negative projected relative streamflow changes ($N_{negative}$) to the number of all simulations ($N = 504$ in this case).

RESULTS AND DISCUSSION

Performance of the HM

Evaluation statistics in Table 3 indicate good model performances forced by the observed climate variables: daily Nash–Sutcliffe coefficients (*NS*) (Nash & Sutcliffe 1970) larger than 0.8 and percent biases (*PBIAS*) within ±10% (Table 3) for both calibration and validation periods. For the high flow and low flow, '*PBIAS*'s of the 3DMHF and 7DMLF are −19.6% and 7.5%, respectively, during 1990–2002. The validation period is three times longer than the calibration period, indicating the calibrated HM is robust, and therefore could be used to study the impact of climate change on local hydrological processes.

Figure 3 compares observed streamflow series, and simulated streamflow series driven by observed meteorological inputs and bias-corrected GCM outputs (combinations of 21 GCMs, 4 'BC_{pcp}'s and 3 'BC_{tmp}'s) in the control period. The 90% percentile (shaded) of simulated streamflow driven with bias-corrected GCM outputs bracketed both the monthly average observations (left plot) and the observed streamflows at each exceedance (right plot). In

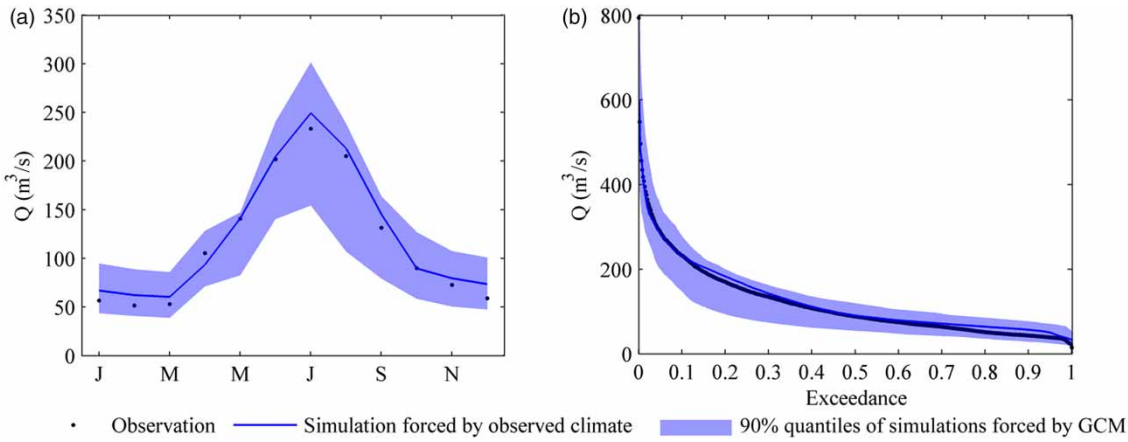

Figure 3 | Observed (dots) and simulated streamflows forced by the observed meteorological data (lines) and bias-corrected GCM outputs (shaded area representing 90% percentile) for the control period: (a) monthly average streamflows and (b) exceedance probability curve of the streamflows.

addition, '*PBIAS*'s for 3DMHF and 7DMLF ranged from −39.4% to 77.6% and −55.5% to 150.4% with 67% and 34% of these simulations having absolute *PBIAS* values within 20%. The model performances show generally satisfactory results and could be used to study the impact of climate change.

Projected changes in the precipitation and temperature

The projected precipitation and temperature changes are presented in Figure 4. The medians of annual precipitation change are 8% and 16%, while their 25% and 75% quantiles are 3.1%–18% and 7.0%–22.5% under RCP4.5 and RCP8.5, respectively, for 2080–2099. There is a significant seasonal variation in the precipitation change with a substantial increase in the cold season (November to April of the next year) and small increase during summer (June, July and August) with large differences among GCMs. The uncertainty bands of projected precipitation gradually increases throughout the 21st century.

For temperature, all GCMs projected a continuous increasing trend with the median increasements being 3.6 °C and 6.5 °C, and their 25% and 75% quantiles ranging from 2.0 °C to 3.3 °C and 4.2 °C to 5.5 °C, respectively, under RCP4.5 and RCP8.5 for 2080–2099 (Figure 4). Compared to precipitation, uncertainty in temperature projections are considerably smaller.

Projected streamflow change

Changes in streamflow volume and timing

Changes in the precipitation and temperature led to changes in the streamflow. The following results are based on 504 simulations forced by all combinations of RCPs, GCMs, BC_{tmp} and BC_{pcp}. Figure 4 shows the streamflow changes with their 25% and 75% quantiles. This indicates there is no general conclusion that these changes are definitely positive or negative or have the same magnitude. The largest decrease will be likely to occur during 2080–2099 under RCP8.5. The medians of annual streamflow change are −12.5% and −18%, while their 25% and 75% quantiles are −26% to 3.4% and −38% to −7% under RCP4.5 and RCP8.5, respectively, for 2080–2099. Note that most models project decreasing streamflow after the 2060s due to the continuously rising temperature. Seasonally, monthly average streamflow decreases by 15% and 27% for the summer season (June, July and August) while it increases

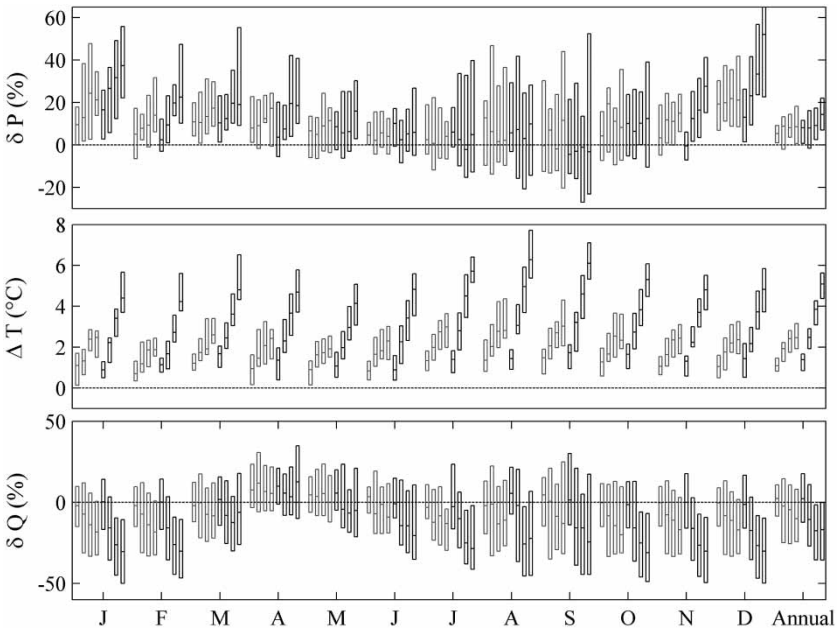

Figure 4 | GCM projected monthly precipitation change (δP), temperature change (ΔT) at the Bayanbulak station, and projected streamflow change (δQ) under RCP4.5 (grey) and RCP8.5 (black) for the four periods in the 21st century (four boxes sequentially).

by 3.0% and 3.7% for spring (March, April and May) under RCP4.5 and RCP8.5 in 2080–2099.

In a previous study conducted in the Kaidu River Basin, Liu *et al.* (2011) reached the conclusion that the qualitative impact results were highly consistent, while they are not in our case. As we used 21 GCMs and different bias correction methods, the climate change scenarios were expected to have larger ranges. This is further discussed based on credibility and consistency indices in the text below. Differences can also be found in the streamflow projections during the snow melt period. Liu *et al.* (2011) concluded that the flow changes are strongly positive during April–May (17.7%–29.7%) for 2046–2065 using a lumped conceptual model (VHM). Our conclusion is comparable to Liu *et al.* (2011) and Fang *et al.* (2015a), but with larger width (−8.3% to 30.6% under RCP4.5 and −18.4% to 23.6% under RCP8.5 during the counterpart period). The reason may be related to the fact that multiple bias correction methods were used in our study while only one (a perturbation approach, equivalent to QM) was used in Liu *et al.* (2011). The decrease in summer runoff has been supported in many other regions, e.g., the Aksu River in south Tienshan Mountains (Duethmann *et al.* 2016), a forested Canadian watershed (Chen *et al.* 2011), the midlatitude alpine regions of the Swiss Alps (Addor *et al.* 2014) and the Colorado River Basin (Christensen & Lettenmaier 2007).

Changes in high flows and low flows

Future changes in high flows and low flows represented by 3DMHF and 7DMLF are shown in Figure 5. The median changes in the high flows for different exceedances are projected to range from −8.5% to 17.4%, while those in low flow will decrease by 12.4% to 46.7%, which may result in potential drought and hinder agriculture irrigation for the oasis in the lower reaches, especially under RCP8.5. We should be careful when interpreting changes in the low flows as only 32% of the simulations have absolute *PBIAS* values within 20% for the control period. For the high flow, the extremely high flood, e.g., exceedance <0.1, will not have a significantly increasing trend, while the relatively small peaks with exceedance between 0.8 and 1.0 will increase, which may help ecological recovery in the lower reaches of the Kaidu River. Many previous studies (Ragettli *et al.* 2016; Zhang *et al.* 2016) concluded that the extreme flow has been increasing or will increase in many mountainous regions, e.g., the Aksu River Basin amd the Langtang River. This may be related to these rivers having a considerable part of the runoff fed by glacier melt water, while the

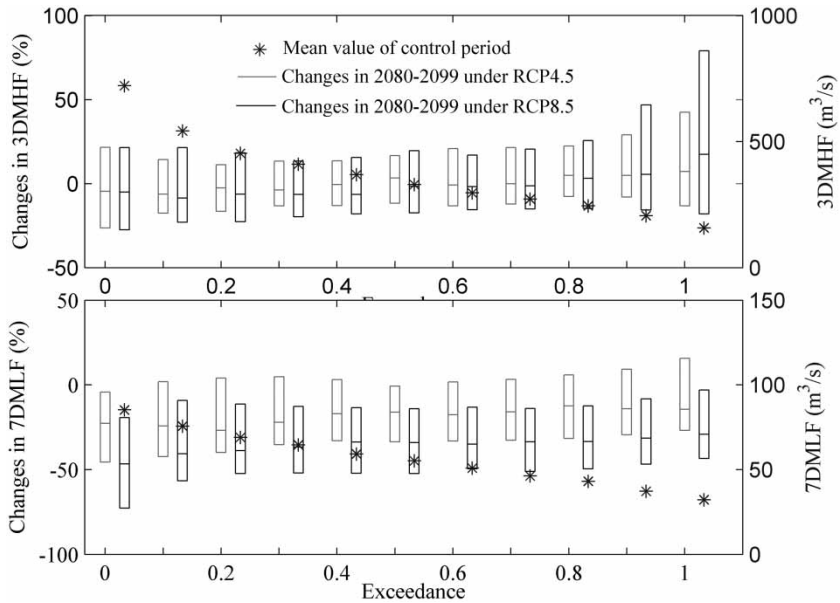

Figure 5 | Projected changes in high and low flows under RCP4.5 (grey) and RCP8.5 (black) for 2080–2099 compared to the control period, whose values are shown as black stars on the right axis.

contribution of glacier melt to runoff in the Kaidu River basin is approximately 10%, which cannot generate a severe flood under a warmer climate.

Changes in hydrological components

Figure 6 shows the projected changes in SM, surface streamflow (R_s), subsurface streamflow (R_g) and evapotranspiration (ET) for 2080–2099 under RCP8.5 (changes in the hydrological components under RCP4.5 (also shown) are similar but smaller and not discussed here). The changes exhibit an obvious seasonality, i.e., insignificant from October to March and significant from April to September during which SM and rainfall occur. SM increases by 16% and 18% in March to May and 49% and 79% in June to August under RCP4.5 and RCP8.5, respectively, for 2080–2099. The contribution of SM to streamflow will decrease from 0.22 for the control period to 0.19 and 0.17 for 2080–2099 under RCP4.5 and RCP8.5, respectively, which means that SM is decreasing in importance. The snow melting time will shift forward approximately 1–2 months. This shifting may be partially attributed to the increased temperature, which governs snow melt, as demonstrated by other studies (Barnett *et al.* 2005; Moore *et al.* 2007). R_s will shift forward with more water generated during March to May and less water during June to August. Changes in the annual R_g are insignificant (4%–5%), which indicates the groundwater flow is the most stable component. ET will increase throughout the 21st century with a median increment of 24%–42%.

Uncertainty decomposition

Table 4 lists uncertainty contributions of streamflow from GCMs, RCPs, BC_{pcp} and BC_{tmp} using the standard deviation method and the ANOVA approach. For both methods, GCMs is the most important uncertainty source in streamflow projection, which coincides with previous studies (Buytaert *et al.* 2010; Chen *et al.* 2011; Bosshard *et al.* 2013). Based on the standard deviation method, all contributions increase over these four periods slightly, e.g., contributions related to GCMs and RCPs increased from 0.215 and 0.093 during 2020–2049 to 0.345 and 0.124 during 2080–2099, respectively, indicating that the uncertainties from each source have increased (Wilby & Harris 2006; Exbrayat *et al.* 2014). Based on ANOVA, GCMs dominates the uncertainty with its contributions ranging from 0.907 to 0.967,

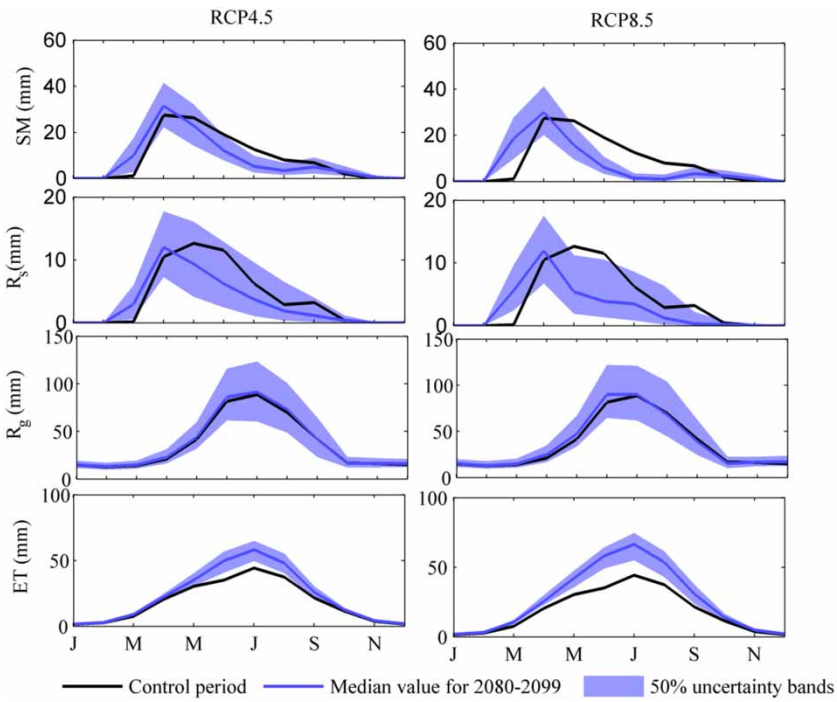

Figure 6 | Monthly average values of SM, surface streamflow (R_s), subsurface streamflow (R_g) and ET for the control period (black line) and 2080–2099 with 50% uncertainty bands.

Table 4 | Period average of uncertainty decomposition based on standard deviation method and ANOVA

	Standard deviation method				ANOVA			
	GCM	RCP	BC_{pcp}	BC_{tmp}	GCM	RCP	BC_{pcp}	BC_{tmp}
2020–2039	0.215	0.093	0.061	0.036	0.947	0.033	0.017	0.003
2040–2059	0.300	0.094	0.082	0.038	0.967	0.009	0.023	0.001
2060–2079	0.303	0.110	0.098	0.042	0.907	0.053	0.035	0.005
2080–2099	0.345	0.124	0.115	0.049	0.943	0.014	0.039	0.004
Average	0.291	0.105	0.089	0.041	0.941	0.027	0.028	0.003

while other sources can be ignored. The uncertainty proportion of GCM or RCP did not show an obvious increase with time based on ANOVA, which is different from Wilby & Harris (2006).

The uncertainty from GCMs based on the standard deviation method is the most important, which accounts for 55.3% of the total uncertainty, which is much lower than that based on the ANOVA approach (over 90% uncertainty caused by the GCMs). The reason may be that the ANOVA uses the *square index* to quantify the uncertainty contribution, which tends to favour high uncertainty sources.

The uncertainty result demonstrates the high contribution of climate models in uncertainty estimation of streamflow and suggests that the most effective way to reduce projection uncertainty is to reduce uncertainties in climatic predictions, as shown in Zhang *et al.* (2015).

As uncertainty in hydrological modelling is inevitable, it is important to determine the credibility and robustness of the projected streamflow change. Here, we used signal-to-noise ratio (*S/N*) (Zhou & Yu 2006; Addor *et al.* 2014) to represent this credibility. The median S/N for 2080–2099 is only 0.214 and 0.246 (less than 1) for RCP4.5 and RCP8.5 (Figure 7), respectively. Higher credibility was found in winter months (January, February, November and December) and SM season (April) under RCP8.5, indicating

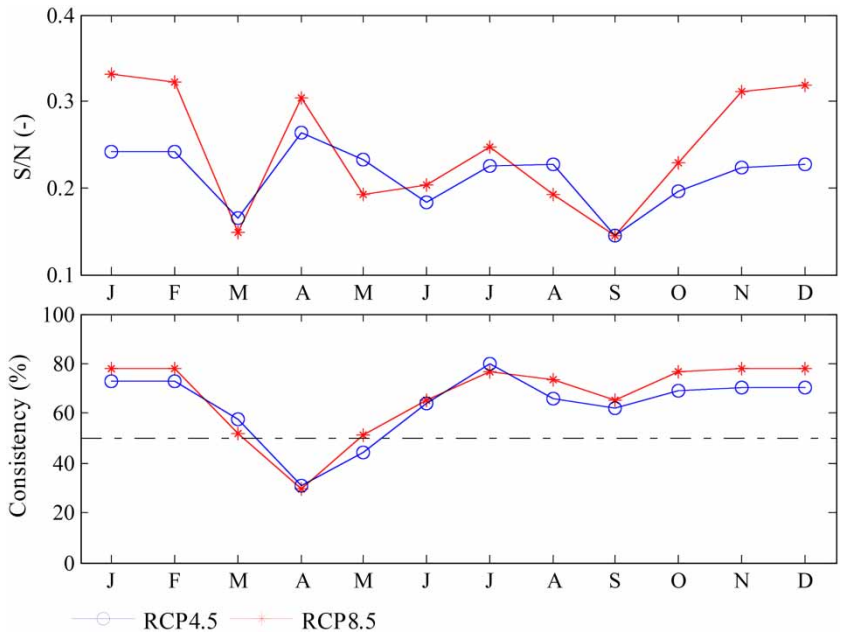

Figure 7 | The signal-to-noise ratio (*S/N*) (top) and consistencies (bottom) based on the projected streamflows in 2080–2099 under RCP4.5 and RCP8.5.

that the projection has higher credibility in these months compared to other months.

Furthermore, the consistency is estimated based on 504 simulations. Approximately 63.4% and 66.9% of the simulations demonstrate a negative streamflow change in 2080–2099 under RCP4.5 and RCP8.5 compared to 1986–2005. Most simulations (70.0% and 74.4%) show decreasing trends during June to February in the next year while only 30.9% and 29.4% of the simulations show a decreasing trend in April for these two scenarios. The S/N and consistency results both suggest that the streamflows are likely to increase in April and decrease in winter months, and for other months the changes are with high uncertainty, thus caution needs to be taken when used for decision-making.

CONCLUSIONS

In this study, we analysed the climate change impacts on hydrological processes for an important headwater of the Tarim River Basin with uncertainty analysis. A well-calibrated SWAT model forced by the downscaled and bias-corrected outputs of 21 GCMs was applied to investigate the effects of climate change on hydrological processes and the impact of GCM structural uncertainty on the hydrological processes.

While all the state-of-the-art GCMs predicted an increased temperature, the predicted precipitation has both decreasing and increasing trends of different magnitudes. Precipitation will increase by 3.1%–18% and 7.0%–22.5% while temperature will increase by 2.0 °C–3.3 °C and 4.2 °C–5.5 °C (represented by their 25% and 75% quantiles), respectively, for 2080–2099 under RCP4.5 and RCP8.5.

For the 21st century, streamflow is likely to increase until the 2060s and then decrease thereafter. Streamflow will change by −26% to 3.4% under RCP4.5 and by −38% to −7% under RCP8.5, respectively, for 2080–2099. Seasonally, streamflow will decrease by −27% and −15% for the summer months (June, July and August), while it will increase by 3.0% and 3.7% in spring (March, April and May) under RCP4.5 and RCP8.5, which may result in a potential water shortage during the critical water-demand summer. The seasonal shift of streamflow may be related to the spring freshet because SM will shift forward for approximately 1–2 months.

GCMs-related uncertainty was the most important based on the standard deviation method and ANOVA approach, while uncertainties linked to RCPs and bias corrections for precipitation and temperature are less important. The standard deviation method generated more mediocre results compared to the ANOVA approach.

Although the impacts of climate change on hydrological processes have been investigated in many previous studies, this study presents a complete study on future hydrological changes, highlighting the uncertainties caused by climate models. This study provides useful information on predicting uncertainty and credibility for water resource management and agricultural planning.

ACKNOWLEDGEMENTS

The research was supported by the 'Thousand Youth Talents' Plan (Xinjiang Project Y371051), the National Natural Science Foundation of China (41630859) and the CAS 'Light of West China' Program (2016-QNXZ-B-12).

REFERENCES

Addor, N., Rössler, O., Köplin, N., Huss, M., Weingartner, R. & Seibert, J. 2014 Robust changes and sources of uncertainty in the projected hydrological regimes of Swiss catchments. *Water Resources Research* **50**, 7541–7562.

Arnold, J. G., Srinivasan, R., Muttiah, R. S. & Williams, J. 1998 Large area hydrologic modeling and assessment part I: model development. *JAWRA Journal of the American Water Resources Association* **34** (1), 73–89.

Awan, U. K., Liaqat, U. W., Choi, M. & Ismaeel, A. 2016 A SWAT modeling approach to assess the impact of climate change on consumptive water use in Lower Chenab Canal area of Indus basin. *Hydrology Research* **47** (5), 1025–1037.

Barnett, T. P., Adam, J. C. & Lettenmaier, D. P. 2005 Potential impacts of a warming climate on water availability in snow-dominated regions. *Nature* **438** (7066), 303–309.

Benestad, R. E. 2004 Tentative probabilistic temperature scenarios for Northern Europe. *Tellus A* **56** (2), 89–101.

Block, P. J., Souza Filho, F. A., Sun, L. & Kwon, H. H. 2009 A streamflow forecasting framework using multiple climate and hydrological models. *JAWRA Journal of the American Water Resources Association* **45**, 828–843.

Booij, M. J. 2005 Impact of climate change on river flooding assessed with different spatial model resolutions. *Journal of Hydrology* **303**, 176–198.

Bosshard, T., Carambia, M., Goergen, K., Kotlarski, S., Krahe, P., Zappa, M. & Schär, C. 2013 Quantifying uncertainty sources in an ensemble of hydrological climate-impact projections. *Water Resources Research* **49** (3), 1523–1536.

Buytaert, W., Vuille, M., Dewulf, A., Urrutia, R., Karmalkar, A. & Celleri, R. 2010 Uncertainties in climate change projections and regional downscaling in the tropical Andes: implications for water resources management. *Hydrology and Earth System Sciences* **14** (7), 1247–1258.

Chen, Y. 2014 *Water Resources Research in Northwest China*. Springer, Dordrecht, The Netherlands.

Chen, J., Brissette, F. P., Poulin, A. & Leconte, R. 2011 Overall uncertainty study of the hydrological impacts of climate change for a Canadian watershed. *Water Resources Research* **47** (12), W12509.

Chen, H., Xu, C. Y. & Guo, S. 2012 Comparison and evaluation of multiple GCMs, statistical downscaling and hydrological models in the study of climate change impacts on runoff. *Journal of Hydrology* **434**, 36–45.

Chen, J., Brissette, F. P., Chaumont, D. & Braun, M. 2013 Performance and uncertainty evaluation of empirical downscaling methods in quantifying the climate change impacts on hydrology over two North American river basins. *Journal of Hydrology* **479**, 200–214.

Chen, J., Brissette, F. P. & Lucas-Picher, P. 2016 Transferability of optimally-selected climate models in the quantification of climate change impacts on hydrology. *Climate Dynamics* **47**, 3359–3372.

Christensen, N. S. & Lettenmaier, D. P. 2007 A multimodel ensemble approach to assessment of climate change impacts on the hydrology and water resources of the Colorado River Basin. *Hydrology and Earth System Sciences* **11**, 1417–1434.

Déqué, M., Somot, S., Sanchez-Gomez, E., Goodess, C., Jacob, D., Lenderink, G. & Christensen, O. 2012 The spread amongst ENSEMBLES regional scenarios: regional climate models, driving general circulation models and interannual variability. *Climate Dynamics* **38**, 951–964.

Dobler, C., Hagemann, S., Wilby, R. L. & Stoetter, J. 2012 Quantifying different sources of uncertainty in hydrological projections in an Alpine watershed. *Hydrology and Earth System Sciences* **16** (11), 4343–4360.

Duethmann, D., Menz, C., Jiang, T. & Vorogushyn, S. 2016 Projections for headwater catchments of the Tarim River reveal glacier retreat and decreasing surface water availability but uncertainties are large. *Environmental Research Letters* **11**, 054024.

Exbrayat, J. F., Buytaert, W., Timbe, E., Windhorst, D. & Breuer, L. 2014 Addressing sources of uncertainty in runoff projections for a data scarce catchment in the Ecuadorian Andes. *Climatic Change* **125**, 221–235.

Fang, G., Yang, J., Chen, Y., Zhang, S., Deng, H., Liu, H. & De Maeyer, P. 2015a Climate change impact on the hydrology of a typical watershed in the Tianshan Mountains. *Advances in Meteorology* **2015**, 1–10.

Fang, G. H., Yang, J., Chen, Y. N. & Zammit, C. 2015b Comparing bias correction methods in downscaling meteorological variables for a hydrologic impact study in an arid area in China. *Hydrology and Earth System Sciences* **19** (6), 2547–2559.

Fang, G., Yang, J., Chen, Y., Xu, C. & De Maeyer, P. 2015c Contribution of meteorological input in calibrating a distributed hydrologic model in a watershed in the Tianshan Mountains, China. *Environmental Earth Sciences* **74** (3), 2413–2424.

Ficklin, D. L., Stewart, I. T. & Maurer, E. P. 2013 Climate change impacts on streamflow and subbasin-scale hydrology in the Upper Colorado River Basin. *PLoS One* **8** (8), e71297.

Finger, D., Heinrich, G., Gobiet, A. & Bauder, A. 2012 Projections of future water resources and their uncertainty in a glacierized catchment in the Swiss Alps and the subsequent effects on hydropower production during the 21st century. *Water Resources Research* **48**, W02521.

Gampe, D., Nikulin, G. & Ludwig, R. 2016 Using an ensemble of regional climate models to assess climate change impacts on water scarcity in European river basins. *Science of the Total Environment* **573**, 1503–1518.

Graham, L. P., Hagemann, S., Jaun, S. & Beniston, M. 2007 On interpreting hydrological change from regional climate models. *Climatic Change* **81**, 97–122.

Hagemann, S., Chen, C., Clark, D. B., Folwell, S., Gosling, S. N., Haddeland, I., Hanasaki, N., Heinke, J., Ludwig, F., Voss, F. & Wiltshire, A. J. 2013 Climate change impact on available water resources obtained using multiple global climate and hydrology models. *Earth System Dynamics* **4**, 129–144.

Horton, P., Schaefli, B., Mezghani, A., Hingray, B. & Musy, A. 2006 Assessment of climate-change impacts on alpine discharge regimes with climate model uncertainty. *Hydrological Processes* **20**, 2091–2109.

Huss, M., Zemp, M., Joerg, P. C. & Salzmann, N. 2014 High uncertainty in 21st century runoff projections from glacierized basins. *Journal of Hydrology* **510**, 35–48.

IPCC 2013 *The Physical Science Basis. Contribution of Working Group I to the Fifth Assessment Report of the Intergovernmental Panel on Climate Change*. Cambridge, UK and New York, USA, 1552 pp.

IPCC 2014 *Climate Change 2014: Impacts, Adaptation, and Vulnerability. Part A: Global and Sectoral Aspects. Contribution of Working Group II to the Fifth Assessment Report of the Intergovernmental Panel on Climate Change*. Cambridge University Press, Cambridge, UK and New York, USA, 1132 pp.

Jayakrishnan, R., Srinivasan, R., Santhi, C. & Arnold, J. 2005 Advances in the application of the SWAT model for water resources management. *Hydrological Processes* **19** (3), 749–762.

Jiang, T., Chen, Y. D., Xu, C., Chen, X., Chen, X. & Singh, V. P. 2007 Comparison of hydrological impacts of climate change

simulated by six hydrological models in the Dongjiang Basin, South China. *Journal of Hydrology* **336**, 316–333.

Lenderink, G., Buishand, A. & Deursen, W. 2007 Estimates of future discharges of the river Rhine using two scenario methodologies: direct versus delta approach. *Hydrology and Earth System Sciences* **11**, 1145–1159.

Li, P., Qian, H., Howard, K. W. F. & Wu, J. 2015 Building a new and sustainable 'Silk Road economic belt'. *Environmental Earth Sciences* **74**, 7267–7270.

Liu, Z., Xu, Z., Huang, J., Charles, S. P. & Fu, G. 2010 Impacts of climate change on hydrological processes in the headwater catchment of the Tarim River basin, China. *Hydrological Processes* **24** (2), 196–208.

Liu, T., Willems, P., Pan, X. L., Bao, A. M., Chen, X., Veroustraete, F. & Dong, Q. H. 2011 Climate change impact on water resource extremes in a headwater region of the Tarim basin in China. *Hydrology and Earth System Sciences* **15** (11), 3511–3527.

Lung, T., Dosio, A., Becker, W., Lavalle, C. & Bouwer, L. M. 2013 Assessing the influence of climate model uncertainty on EU-wide climate change impact indicators. *Climatic Change* **120**, 211–227.

Lutz, A. F., Immerzeel, W. W., Gobiet, A., Pellicciotti, F. & Bierkens, M. F. P. 2013 Comparison of climate change signals in CMIP3 and CMIP5 multi-model ensembles and implications for Central Asian glaciers. *Hydrology and Earth System Sciences* **17**, 3661–3677.

Moore, J. N., Harper, J. T. & Greenwood, M. C. 2007 Significance of trends toward earlier snowmelt runoff, Columbia and Missouri Basin headwaters, western United States. *Geophysical Research Letters* **34** (16), L16402.

Nash, J. E. & Sutcliffe, J. 1970 River flow forecasting through conceptual models part I – a discussion of principles. *Journal of Hydrology* **10** (3), 282–290.

Piani, C., Weedon, G. P., Best, M., Gomes, S. M., Viterbo, P., Hagemann, S. & Haerter, J. O. 2010 Statistical bias correction of global simulated daily precipitation and temperature for the application of hydrological models. *Journal of Hydrology* **395**, 199–215.

Piao, S., Ciais, P., Huang, Y., Shen, Z., Peng, S., Li, J., Zhou, L., Liu, H., Ma, Y. & Ding, Y. 2010 The impacts of climate change on water resources and agriculture in China. *Nature* **467** (7311), 43–51.

Ragettli, S., Pellicciotti, F., Bordoy, R. & Immerzeel, W. W. 2013 Sources of uncertainty in modeling the glaciohydrological response of a Karakoram watershed to climate change. *Water Resources Research* **49**, 6048–6066.

Ragettli, S., Immerzeel, W. W. & Pellicciotti, F. 2016 Contrasting climate change impact on river flows from high-altitude catchments in the Himalayan and Andes Mountains. *Proceedings of the National Academy of Sciences* **113**, 9222–9227.

Reyers, M., Pinto, J. G. & Paeth, H. 2013 Statistical–dynamical downscaling of present day and future precipitation regimes in the Aksu river catchment in Central Asia. *Global and Planetary Change* **107**, 36–49.

Rumbaur, C., Thevs, N., Disse, M., Ahlheim, M., Brieden, A., Cyffka, B., Duethmann, D., Feike, T., Frör, O., Gärtner, P., Halik, Ü., Hill, J., Hinnenthal, M., Keilholz, P., Kleinschmit, B., Krysanova, V., Kuba, M., Mader, S., Menz, C., Othmanli, H., Pelz, S., Schroeder, M., Siew, T. F., Stender, V., Stahr, K., Thomas, F. M., Welp, M., Wortmann, M., Zhao, X., Chen, X., Jiang, T., Luo, J., Yimit, H., Yu, R., Zhang, X. & Zhao, C. 2015 Sustainable management of river oases along the Tarim River (SuMaRiO) in Northwest China under conditions of climate change. *Earth System Dynamics* **6** (1), 83–107.

Sanborn, S. C. & Bledsoe, B. P. 2006 Predicting streamflow regime metrics for ungauged streams in Colorado, Washington, and Oregon. *Journal of Hydrology* **325**, 241–261.

Schmidli, J., Frei, C. & Vidale, P. L. 2006 Downscaling from GC precipitation: a benchmark for dynamical and statistical downscaling methods. *International Journal of Climatology* **26**, 679–689.

Shi, Y., Shen, Y., Kang, E., Li, D., Ding, Y., Zhang, G. & Hu, R. 2007 Recent and future climate change in northwest China. *Climatic Change* **80** (3–4), 379–393.

Shrestha, B., Cochrane, T. A., Caruso, B. S., Arias, M. E. & Piman, T. 2016 Uncertainty in flow and sediment projections due to future climate scenarios for the 3S Rivers in the Mekong Basin. *Journal of Hydrology* **540**, 1088–1104.

Singh, H. V., Kalin, L., Morrison, A., Srivastava, P., Lockaby, G. & Pan, S. 2015 Post-validation of SWAT model in a coastal watershed for predicting land use/cover change impacts. *Hydrology Research* **46**, 837–853.

Sorg, A., Bolch, T., Stoffel, M., Solomina, O. & Beniston, M. 2012 Climate change impacts on glaciers and runoff in Tien Shan (Central Asia). *Nature Climate Change* **2** (10), 725–731.

Tamm, O., Luhamaa, A. & Tamm, T. 2016 Modeling future changes in the North-Estonian hydropower production by using SWAT. *Hydrology Research* **47**, 835–846.

Terink, W., Hurkmans, R., Torfs, P. & Uijlenhoet, R. 2010 Evaluation of a bias correction method applied to downscaled precipitation and temperature reanalysis data for the Rhine basin. *Hydrology & Earth System Sciences* **14**, 687–703.

Teutschbein, C. & Seibert, J. 2012 Bias correction of regional climate model simulations for hydrological climate-change impact studies: review and evaluation of different methods. *Journal of Hydrology* **456**, 12–29.

Themeßl, M. J., Gobiet, A. & Heinrich, G. 2012 Empirical-statistical downscaling and error correction of regional climate models and its impact on the climate change signal. *Climatic Change* **112**, 449–468.

Van Vuuren, D. P., Edmonds, J., Kainuma, M., Riahi, K., Thomson, A., Hibbard, K., Hurtt, G. C., Kram, T., Krey, V. & Lamarque, J.-F. 2011 The representative concentration pathways: an overview. *Climatic Change* **109**, 5–31.

Vidal, J. P., Hingray, B., Magand, C., Sauquet, E. & Ducharne, A. 2016 Hierarchy of climate and hydrological uncertainties in

transient low-flow projections. *Hydrology and Earth System Sciences* **20**, 3651–3672.

Wilby, R. L. & Harris, I. 2006 A framework for assessing uncertainties in climate change impacts: low-flow scenarios for the River Thames, UK. *Water Resources Research* **42**, W02419.

Xu, C. & Xu, Y. 2012 The projection of temperature and precipitation over China under RCP scenarios using a CMIP5 multi-model ensemble. *Atmospheric and Oceanic Science Letters* **5** (6), 527–533.

Xu, C., Zhao, J., Deng, H., Fang, G., Tan, J., He, D., Chen, Y., Chen, Y. & Fu, A. 2016 Scenario-based runoff prediction for the Kaidu River basin of the Tianshan Mountains, Northwest China. *Environmental Earth Sciences* **75**, 1126.

Yip, S., Ferro, C. A., Stephenson, D. B. & Hawkins, E. 2011 A simple, coherent framework for partitioning uncertainty in climate predictions. *Journal of Climate* **24**, 4634–4643.

Zhang, Y., Su, F., Hao, Z., Xu, C., Yu, Z., Wang, L. & Tong, K. 2015 Impact of projected climate change on the hydrology in the headwaters of the Yellow River basin. *Hydrological Processes* **29**, 4379–4397.

Zhang, Q., Gu, X. H., Singh, V. P., Sun, P., Chen, X. H. & Kong, D. D. 2016 Magnitude, frequency and timing of floods in the Tarim River basin, China: changes, causes and implications. *Global and Planetary Change* **139**, 44–55.

Zhou, T. & Yu, R. 2006 Twentieth-century surface air temperature over China and the globe simulated by coupled climate models. *Journal of Climate* **19**, 5843–5858.

First received 12 September 2016; accepted in revised form 6 March 2017. Available online 21 April 2017